



EUROPEAN ORGANIZATION FOR NUCLEAR RESEARCH

CERN/ISR-BOM-OP/82-19

PREPARATION OF THE OPERATION OF THE SUPERCONDUCTING LOW- β INSERTION IN THE ISR

by

T. Risselada and A. Verdier

Abstract

The low- β insertion described in Ref. 1 was installed in intersection 8 of the ISR in 1980, and has been operated successfully since.

This report describes the modifications to the scheme in Ref. 1 which were found to be necessary before operation as well as the new procedures which have been created to make the operation possible.

Geneva, Switzerland

December 1982

Contents

INTRODUCTION

1. MODIFICATIONS TO THE SCHEME OF REF. 1
 - 1.1 Effect of the displacement of the SL insertion from I1 to I8
 - 1.2 Modification due to the SL end effects
 - 1.3 Modification of the compensation scheme for the AFM
 - 1.4 Expected performances of the new scheme compared to those given in Ref. 1

2. NEW PROCEDURES FOR OPERATION OF THE SL MACHINE
 - 2.1 Changes to the collimator system
 - 2.2 Modification of the program QPQQ which adjusts the tunes of the ISR
 - 2.3 Space charge compensation
 - 2.4 Beam centring
 - 2.5 Local correction of the dipole field defect in the insertion
 - 2.6 Initial set up of the injection with minimum risk of losses in I8
 - 2.7 Fast injection procedure on a known closed orbit

3. BETATRON MATCHING OF THE BEAM TRANSFER LINE TO THE ISR

REFERENCES

APPENDIX 1

APPENDIX 2

APPENDIX 3

APPENDIX 4

APPENDIX 5

TABLES 4 a - 4 d

FIGURES



INTRODUCTION

After the approval of the project of a superconducting low- β insertion (SL insertion) for the ISR in 1977, based on the scheme shown in Ref. 1, some modifications were made:

- i) It was decided to install the SL insertion in intersection 8 instead of intersection 1, which had consequences on the luminosity balance.
- ii) The end effects of the SL quadrupoles were taken into consideration and the matching of the insertion was remade accordingly.
- iii) The calculation of the off-momentum closed orbits in the program AGS was improved²⁾, which necessitated the recalculation of the sextupole components in the insertion.

These modifications are described in the first chapter of this report.

The second chapter describes the new procedures and items specially created for the SL operation, they are:

- i) A program which uses trajectory measurements and corrects locally the dipole defects of the insertion as well as its phase jump.
- ii) A special data base for the program QPQQ which is used to tune the machine.
- iii) An improved beam centring procedure.
- iv) A collimator system adapted to the SL operation.

In the third chapter a new method of matching the ISR transfer line is described, which takes into account the actual betatron parameters in the injection septum.

1. MODIFICATIONS TO THE SCHEME OF REF.1

1.1 Effect of the displacement of the SL insertion from I1 to I8

The magnet parameters and the luminosity computed in Ref. 1 assumed the installation of the insertion in I1.

Installing the insertion in I8 did not change the SL magnet parameters. The betatron functions which are necessary for matching are in fact the same in all intersections of the ISR.

However, because of the modulation of the function β_h due to the horizontal mismatch of the insertion, the β_h values at the inflectors are different in the I8 case from what they were in the I1 case. This reduces the available aperture

in ring 1 and increases it in ring 2. The relevant β_h values are given in Table 1.

Table 1

Location of insertion	I1 (ring 1 & 2)	I8 (ring 1)	I8 (ring 2)
$\beta_h(m)$ at the injection kicker on the injection orbit	65.5	111	8.3

The reduction of luminosity due to this change was expected to be about 7 %, the aperture balance being made as in Ref. 1, however this was considered to be the price to pay for the change of the initial design.

1.2 Modification due to the SL end effects

In Ref. 1 the SL quadrupoles and sextupole components were described as having a constant value inside the magnets and a zero value outside. In reality the value of these components decreases smoothly at the ends of the magnets³⁾. The influence of this variation on the β_v^* function was examined some time ago⁴⁾ and was found to be negligible. However the main effect of this variation is the mismatch of the dispersion function which is introduced by the gradient decrease; the associated modulation of the off-momentum closed orbits reduces the stacking aperture by about 6 %. On the other hand the increase of β_v^* is about 8 % which is larger than previously⁴⁾ calculated, since the value of Q_v is closer to 9 for the present scheme.

1.2.1 Model to describe the end effects

The decrease of the gradient at the end of the magnet was extracted from Ref. 3. It is shown in Fig. 1 for two radial positions. The similarity of the two curves shows that this representation is valid in the useful aperture.

As the program AGS⁵⁾ only uses piece wise constant components, the end of the quadrupoles, whose length is 0.175 m in the hard edge model, has been replaced by six pieces, 0.055 m long, whose gradients divided by the central gradient gives the numbers:

$$0.927 \quad 0.841 \quad 0.688 \quad 0.459 \quad 0.210 \quad 0.05682$$

This is illustrated by Fig. 1. This representation guarantees the value of the integrated gradient within 10^{-5} and provides transfer matrices which are very close to the matrices computed by means of a smooth curve as shown in Appendix 1. This representation will be referred to as "smooth edge" model.

1.2.2 Errors due to the hard edge approximation

One way to estimate these errors is to introduce the gradients computed in the hard edge approximation in the smooth edge model. The machine parameters are affected as shown in Table 2 for ring 2 (the situation is similar for ring 1).

Table 2.

Tunes and their derivatives as well as luminosity parameters with insertion gradients computed for the hard edge model (Ring 2)

parameter	Q_h	Q'_h	Q''_h	Q_v	Q'_v	Q''_v	D_{\max} (m)	β^*_v (m)	$\Delta p/p$ stacked (%)
hard edge	8.902	2.55	- 2.98	8.882	2.48	3.62	2.306	0.275	3.87
smooth edge	8.905	2.62	- 6.21	8.870	2.54	7.75	2.363	0.299	3.62

1.2.3 Rematching of the linear scheme

Taking the hard edge gradients as starting values, the previous matching procedure¹⁾ was repeated using only the central part of the quadrupoles as variables and spreading the difference w.r.t. the starting value over the whole magnet.

In practice it was only necessary to do this once, since the solution obtained was quite acceptable, i.e.: good matching of the dispersion, values of the gradient stopbands equal to or lower than those of the hard edge solution (see Table 3 below). The results of the AGS calculations of the β functions, the dispersion and phase advances are shown in Tables 4.a and 4.c. The β functions inside the insertion are shown in Fig. 2.

Table 3

Half widths of the gradient stopbands and maximum value of the dispersion for the hard edge and smooth edge solutions

	δQ_h	δQ_v	D_{\max} (m)	β^*_v (m)
hard edge solution, Ref. 1	0.112	0.008	2.296	0.293
smooth edge ring 1	0.112	0.0034	2.301	0.283
smooth edge ring 2	0.111	0.0060	2.302	0.286

1.2.4 The SL sextupoles for the smooth edge model

The maximisation of the stacking aperture by means of the F sextupoles in the SL quadrupoles was kept as a fundamental principle¹⁾. However as far as the D sextupoles are concerned, the principle of keeping β_V^* constant on the off-momentum orbits¹⁾ has been discarded. Indeed, during the construction and testing of the sextupole windings, it was estimated to be more economic to take the F sextupole component which matches the orbit at the top of the stack as an upper limit, with the accepted consequence of an increase of β_V^* with positive momentum deviation. This results in a luminosity loss of about 4 % w.r.t. a solution with a constant β_V^* .

The decrease of the component at the end of the sextupole has not been computed. It was estimated to be steeper than that of the quadrupole. Thus the decrease of the sextupole component was spread over four of the end quadrupole pieces (see Fig. 1); however this did not significantly affect the variation of β_V^* with momentum or the stacking aperture. In the final scheme the sextupole component was nevertheless described this way for the homogeneity of the representation.

The F components were computed to match the off-momentum closed orbit at the top of the stack (i.e. for $\Delta p/p = 0.021$) and the D components were simply made to equal them. This is an iterative process which necessitated two iterations, starting with the values in Ref. 1. This computation was made with the corrected version of the routine MATRIX in the AGS program²⁾

The detailed procedure is the following:

- Starting values were set for the K' of the sextupoles, the working line was adjusted by means of the K' and K'' components of the main magnets of the ISR (computation made with the MA routine in the AGS⁵⁾ program).
- The insertion was turned off and the off momentum closed orbit position C_m , with the momentum deviation $(\Delta p/p)_m$ desired for matching, was computed.
- A trajectory with the same position and slope as C_m at the beginning of the insertion was tracked for $(\Delta p/p)_m$.
- The difference between this trajectory and C_m at the end of the insertion was made to vanish by adjusting the two F sextupole components.*

* The program SEXT which computes the sextupole components was made by a summer student S. Olivieri in August 1979.

- The procedure was restarted with the new values of the sextupole components.

This is an iterative procedure which converges rather rapidly.

As a consequence of this orbit matching, it must be noted that the AGS⁵⁾ program finds the closed orbits faster when this matching is performed.

The values of the sextupole components are given in the summary of the AGS⁵⁾ outputs for the closed orbits at the top of the stack (Table 4 b and 4 d).

1.3 Modification of the compensation scheme for the AFM

The SL scheme in Ref. 1 was intended to be used with the superconducting solenoid installed in I1. The vertical orbit distortion due to the vertical kick given by the axial field of the solenoid was made local by means of two radial field compensators located at each end of the solenoid.

In I8 the SL insertion had to be used with the open axial field magnet (AFM). As no space was available to install a compensator between the AFM and the SL quadrupole (the AFM pole piece had to be machined to make the installation of the SL quadrupole possible in the outer arc part of the insertion), the compensator of the outer arc had to be put between the two SL quadrupoles in the outer arc. Under these conditions it was advantageous to use the D quadrupoles themselves as compensators.

In order to explain this, let us consider a trajectory starting from the centre of the AFM with a zero slope. This trajectory reaches the D SL quadrupole with a certain vertical position and slope. The strength of the SL quadrupole is such that the maximum excursion of this trajectory occurs in it as shown in Appendix 2. Then the old radial field compensators AFC can be put almost anywhere between the SL quadrupoles and the next H magnet of the ISR to make the position of the trajectory equal to zero at the place of the H magnet. The latter has finally to be powered to give a kick opposite to the slope of the trajectory, which localises the vertical closed orbit distortion.

In practice one AFC is placed inside the doublet in the outer arc and the other one is placed in the free space between the F SL quadrupole and the F magnet of the ISR in the inner arc. Under these conditions the vertical excursion of the closed orbit is smaller than 1.5 mm in the superconducting quadrupoles as well as in the main magnets of the ISR close to the insertion.

This scheme is also convenient for $p\bar{p}$ operation because it provides the same vertical position of the p and \bar{p} beams at the interaction point.

The excitation of the correctors used for this scheme are given in Table 5, as well as increments for a vertical displacement and a change of slope of the vertical closed orbit in I8.

Table 5

Excitation of the AFC's and H's at 26 GeV for the compensation of the vertical kick due to the AFM. Increments of the AFC's and H's for a vertical displacement of the closed orbit and a change of its slope at the interaction point. The kick of the AFM is 0.75 mrad at 26 GeV.

The upper number in each case is the kick in mrad at 26 GeV, the lower number is the intensity in percent of the maximum intensity. The reference axis for the slope is in the direction of the beam. For the H's and AFC's a positive kick corresponds to a positive excitation.

Compensation scheme for + 100 % AFM		-0.06564 -4.48	+0.04017 +3.15	+0.01972 +1.54	-0.06521 -4.46	-0.06568 -4.19	+0.03966 +3.11	+0.00929 +0.73	-0.05800 -3.96
Increments for displacement 1 mm upwards	Angle (mrad)	0.02788	0.33198	0.33146	-0.00523	0.02790	0.33206	0.33297	-0.00455
	Current (%)	+1.91	26.01	25.97	-0.36	1.91	26.01	26.08	-0.31
Increments for + 1 mrad slope change at intersection	Angle (mrad)	-0.17770	+0.07932	-0.01570	+0.1729	-0.17763	0.06882	+0.01190	+0.15376
	Current (%)	-12.14	+5.51	-1.23	+11.81	-12.14	+5.39	+0.93	+10.51

1.4 Expected performances of the new scheme compared to those given in Ref. 1

Three points influence the performance of the new scheme, they are:

- i) The reduction of stacking aperture in ring 1 and its increase in ring 2 result in a luminosity loss of 7 %.
- ii) The limitation of the D-sextupole strengths results in a loss of luminosity of 4 %.
- iii) The decrease of B^* makes the luminosity increase by 1 %.

Thus the number given in Ref. 1 must be decreased by 10 %.

As the expected luminosity was in the range 1 to 3 $10^{32} \text{ cm}^{-2} \text{ s}^{-1}$ depending on the conditions, the statement can be maintained that luminosities in excess of $10^{32} \text{ cm}^{-2} \text{ s}^{-1}$ with an acceptable background for the experiments may be obtained. This was effectively achieved.

2. NEW PROCEDURES FOR SL OPERATION

These new procedures described below can be divided into four groups:

- i) Change of the collimator system for limiting the proton losses in the superconducting quadrupoles.
- ii) Adaptation of the tune control to the SL machine: this control has to be more precise than on the conventional ISR because of the increased sensitivity of the SL machine to vertical field perturbations. This concerns both the QPQQ program and the space charge compensation.
- iii) Special procedure to obtain the first injection on the SL machine and to obtain injection currently with this machine.
- iv) Centring and acceleration.

2.1 Changes to the ISR collimator system

The collimator system had to be adapted to provide maximum protection of the I8 insertion on the SL machine, without losing efficiency on the conventional machines FP, LB and TW.

The efficiency of a collimator configuration⁶⁾ can be evaluated with the programs TOUCH and MUSCAT (see Appendix 5). Betatron phase space plots in the vertical plane show that I8 is protected against any sort of proton losses. However, in the horizontal plane, the phase advances between the existing collimator locations (which should be roughly $\pi/2$ in both planes) are considerably perturbed by the horizontal betatron mismatch introduced by the insertion, and therefore new locations had to be found for some radial collimators, especially to provide a protection for SL7 and SL8.

In ring 2 it was sufficient to displace the farthest downstream collimator 340 (at $3\pi/2$ w.r.t. the primary collimators in I3) to the next straight section 344. This location was equally acceptable on the conventional ISR magnetic machines.

However, in ring 1 the β_h modulation in the collimator region is more visible than in ring 2. The phases of the radial collimators at 241 and 249 are no longer at π and $3\pi/2$ w.r.t. the primary collimators (see Fig. 3 a). To overcome this, a new radial collimator needed to be installed in the straight section 237. Even so, the use of the radial collimator 229 remains delicate, since a large part of the protons scattered by this (farthest downstream) collimator would be lost in the insertion on SL7. Therefore collimator 229 requires continuous attention, and must never be the strongest aperture limitation in the presence of high intensity beams. In the case of a sudden change of the closed orbit or during a coherent instability the beam could scrape itself superficially against the collimator block and the number of outscattered high energy protons would be large, making a quench in SL7 possible.

It was not considered justified to add collimators in the vicinity of I8 (the present collimator system is entirely located around I3), as this would dramatically increase the risk of scattering protons directly onto the superconducting quadrupoles. Furthermore, no equipment possibly causing scattered protons (scrapers, injection kicker, dump, etc.) is located between the present collimator system and the I8 insertion.

The phase space plots of the new configuration show that the superconducting magnets are protected w.r.t. injected pulses as follows:

- in the vertical plane perfectly well,
- in the horizontal plane the ISR vacuum chamber between I3 and I8 protects all magnets except SL7 in ring 1 and SL8 in ring 2, but the collimator system, when set up correctly, protects all magnets against the total loss of a single pulse.

The inner and vertical collimators are positioned by computer (program POCO⁷) around the injection orbit. The outer collimators presently need to be set up manually by "find beam" with a pulse from a position 3 mm further than the top of the stack, starting with the most downstream collimator.

MD tests have shown that, with the collimators in position, the superconducting magnets are protected from quenching during all operation with the exception of the total loss of a high intensity beam. In this event a beam current loss monitor triggers the beam dump. This loss monitor should be set to 1 A/10 seconds (normal value: 2 A/10 s).

2.2 Modification of the program QPQQ adjusting the tunes of the ISR

The program QPQQ computes increments for the currents in the 24 pole face windings of the main magnets of the ISR in order to achieve increments of the tunes and their derivatives.

In practice, these increments are obtained by multiplying a 24 x 10 matrix (10 tunes and derivatives, 24 pole face windings) by a vector constituted by the 10 tunes and derivatives requested. The matrix coefficients were measured some time ago⁸) for the FP machine whose betatron parameters are close to those of the BASE machine, i.e. the machine to which the insertion is matched. Thus a good variation of the tunes will be obtained on the BASE machine by using the FP matrix.

In the SL machine the β'_v 's are the same as for the BASE machine but the β'_h 's are quite different. An alternative way of examining this is to compute the horizontal tune of the SL machine Q_h^* as a function of the horizontal tune of the BASE machine Q_h . This calculation is described in Ref. 9, giving:

$$\cos 2\pi Q_h^* = \cos \pi 2 (Q_h + \phi) / \cos 2\pi Q_h \quad (1)$$

where Q_h is the half width of the gradient stopband associated with the mismatch of the insertion and ϕ is the sum of the phase advance due to the insertion and a term derived from the mismatch.

From equation (1) we can compute the values in Table 6.

Table 6

Horizontal tune of the SL machine Q^*
as a function of the tune of the base machine Q_h

ΔQ_h^*	0	-0.050	-0.01	0.01	0.05	0.098
Q_h^*	8.9020	8.8520	8.8920	8.9120	8.952	9
Q_h	8.7502	8.7184	8.7444	8.7557	8.7733	8.7816
ΔQ_h	0	-0.0318	-0.0058	0.0055	0.0231	0.0314

The non linearity of Q_h^* versus Q_h is clear, Q_h^* is plotted as a function of Q_h on Fig. 4, where the significance of the gradient stopband is explained. The consequence of the non linearity above is that if Q_h is incremented, the associated increment of Q_h^* depends on the value of Q_h . In other words, an increment of Q_h^* made by QPQQ with FP coefficients will also create a variation of its derivatives of Q_h^* versus momentum for the SL machine⁹).

A modification of the QPQQ matrix was made in the following way: using the AGS⁵) program, increments of the multipole components in the main magnets were computed in order to achieve a variation of Q_h^* or of its derivatives; then these increments were added to the components in the main magnets of the FP machine and the associated difference in Q_h and its derivative were computed. In this way it was possible to compose Table 7 which could also be written in a matrix form:

$$[Q(\text{FP})] = [M] [Q(\text{SL})]$$

where $[Q]$ is a vertical vector containing Q and its derivatives.

Table 7

Theoretical conversion of SL increments into FP increments

Increments asked from QPQQ with working conditions FP	Increments wanted for the machine with the SL insertion
$\Delta Q_h =$	$0.535 \Delta Q_h^*$
$\Delta Q'_{h \text{ inner}} =$	$- 7.2 \Delta Q_h^* + 0.58 \Delta Q'_{h \text{ in}} + 0.0006 \Delta Q''_{h}$
$\Delta Q'_{h \text{ outer}} =$	$- 6.4 \Delta Q_h^* + 0.64 \Delta Q'_{h \text{ out}} + 0.0014 \Delta Q''_{h \text{ out}}$
$\Delta Q''_{h \text{ inner}} =$	$-189 \Delta Q_h^* + 11 \Delta Q'_{h \text{ in}} + 0.77 \Delta Q''_{h \text{ in}}$
$\Delta Q''_{h \text{ outer}} =$	$-451 \Delta Q_h^* - 30 \Delta Q'_{h \text{ out}} + 0.17 \Delta Q''_{h \text{ out}}$

Finally the multiplication of the FP QPQQ matrix by the matrix M provides the SL QPQQ matrix. This new matrix was checked experimentally and it was found that some terms had to be adjusted. The experimental results are given in Table 8 for finite increments of Q^* and its derivatives, the non linearity of Q^* versus Q can explain most of the discrepancies between Table 7 and Table 8.

Table 8

Measured coefficients for the conversion of SL tune increments into FP tune increments

Increments asked from QPQQ with working conditions FP	Increments wanted for the machine with the SL insertion
$\Delta Q_h =$	$0.7 \Delta Q_h^*$
$\Delta Q'_{h \text{ inner}} =$	$- 10.0 \Delta Q_h^* + 0.58 \Delta Q'_{h \text{ in}}$
$\Delta Q'_{h \text{ outer}} =$	$- 8.0 \Delta Q_h^* + 0.64 \Delta Q'_{h \text{ out}}$
$\Delta Q''_{h \text{ inner}} =$	$-189 \Delta Q_h^* + 2.0 \Delta Q'_{h \text{ in}} + 0.8 \Delta Q''_{h \text{ in}}$
$\Delta Q''_{h \text{ outer}} =$	$-451 \Delta Q_h^* - 5.0 \Delta Q'_{h \text{ out}} + 0.8 \Delta Q''_{h \text{ out}}$

2.3 Space charge compensation

From the explanations in the above paragraph, it is obvious that the Q-shifts due to the space charge will be more important on the SL machine than in the conventional machines.

However, as the main magnets of the ISR are almost as regularly distributed as the space charge fields, the effect of the space charge can be compensated quasi locally by acting on the main magnets poleface winding currents. The relation between the beam profile (density vs. momentum) and poleface winding current increments then only depends on the current distribution in the vacuum chamber. Since the SL machine was designed to have the same theoretical off-momentum closed orbits as the FP machine outside the insertion, it seemed interesting to use the existing FP space charge compensation procedure equally on the SL machine. The program QCOMP¹⁰⁾, with a modification to select automatically the FP parameters, was found to give adequate results and required only some fine tuning of the parameters FH and FV which multiply the measured current profile before the calculation of the compensation:

FH was increased from + 0.97 (original value) to + 1.11

FV was decreased from - 1.26 (original value) to - 1.40

(the original values were chosen deliberately to undercompensate, which was not desired on the SL machine).

The results of the QCOMP calculations were incorporated into the S.C.C. program TUCO¹¹⁾, which applies precalculated compensations automatically based on the beam current: it uses the position of top and the density of the stack as input parameters and assumes a rectangular distribution. The program TUCO has been used successfully on the SL machine, for the high intensity stacking tests and for the stacks used for acceleration to 31 GeV.

2.4 Beam centring

The compensation of the space charge described just above is also used during beam centring after stacking. On the conventional machine, precalculated increments were used in all cases. However, with the SL machine high precision of the working line handling is essential, therefore as the obtained beam currents and density profiles may be different from one run to the next, a procedure was created to calculate the poleface winding increments "on line" just before centring of the beam, using the QCOMP program with the SHIFT option¹⁰⁾. Application of two steps of 5 mm gave good results and is now regularly used.

2.5 Local correction of the field defects in the insertion

For the running-in of the SL insertion, an essential problem was to inject circulating protons in this new machine.

For this purpose a special procedure was created as follows:

- The ISR was set up on the BASE machine which is obtained in the following way: the ELSA line having been made with the SL insertion, the latter is turned off. The working line then computed with this new machine is the BASE working line.
- The injection on the BASE machine being well adjusted, a single turn trajectory T_1 is measured as well as the closed orbit C_1 at injection.
- The insertion is turned on and a single turn trajectory T_2 is measured.
- Downstream of the insertion the difference between T_2 and T_1 is considered as a betatron oscillation around T_1 . It is eliminated by two dipoles in both planes.
- When the difference between T_2 and T_1 is small enough, the injected pulse circulates; the position of the closed orbit C_2 is measured.
- A fine correction is finally made by cancelling the difference between C_1 and C_2 by means of the same dipoles as above.

This process has two advantages:

- i) It ensures injection on the SL machine.
- ii) It provides a closed orbit at injection as good as the closed orbit made on the base machine, so that the insertion is made invisible from the orbit point of view.

This worked perfectly well with the SL insertion in spite of the bad horizontal matching and made it possible to obtain circulating protons at the first run with the insertion. Fig. 5 shows measurements of the closed orbit distortions measured without the insertion (BASE machine) and with the insertion after having applied INCO on the single turn measurements only (difference between T_2 and T_1 quoted above).

The procedure for using the program INCO can be found in Ref. 12.

The principle of the computations are given in Appendix 4.

2.6 Initial set up of the machine with the insertion

This initial set up had to be carried out with great care because injection attempts before the orbits and injection are properly turned could lead to losses in I8 making the magnets quench.

In order to overcome this problem the beam was not allowed at any time to cross the insertion on an unknown orbit.

At first the set up was made on the BASE machine as defined in § 2.5, identical to the conventional ISR: the working line was adjusted to equal that of the BASE machine with all the ISR magnets needed. The orbits were corrected and the injection line was carefully adjusted. The closed orbit at injection was measured and stored as well as a single turn trajectory. The collimators were positioned w.r.t. the thus measured injection orbit using the β values of the SL machine.

The SL magnets were turned on, the stability of the injection was checked. The injected pulse was then allowed to cross the insertion once and INCO was applied to make the trajectory downstream from the insertion coincide with the orbit measured previously without the SL insertion. When INCO did not require any more correction the beam was allowed to circulate.

This procedure was effectively applied in ring 2 and worked perfectly well (Fig. 5).

In ring 1 the situation differs because I8 is very close to the injection kicker, which invalidates the above procedure. Therefore a second turn trajectory had to be measured and a special kicker was installed in I3 to prevent an injected pulse to cross I8 twice. This was more difficult and lengthy because the injection had to be adjusted frequently due to changes of the PS and the transfer line.

2.7 Fast injection procedure on a known closed orbit

Experience shows that the closed orbits on the SL machine are remarkably stable at 26 GeV/c, and in most cases the closed orbit measured in the previous run is a better estimation of the actual orbit than the closed orbit of the base machine. This fast procedure may however only be applied if no radical realignment work has been carried out since the previous run. The procedure is as follows:

The insertion is switched on together with the other magnets of the machine, and the special stoppers upstream of I8 (449 for ring 1 and 548 for ring 2) are closed to protect the insertion. The injection is tuned (program CINE13) and the collimators are positioned (program POCO⁷) w.r.t. the orbit measurement of the previous run, kept on disk. After taking out the stopper, circulating beam is obtained.

3. BETATRON MATCHING OF THE BEAM TRANSFER LINE TO THE ISR RING

This computation, which is of general interest, was developed for the SL operation because the betatron matching of the beam transfer line to the ISR ring had to be performed with precision; due to the horizontal beta modulation introduced by the insertion, the horizontal beam width is locally much larger than on the conventional machine, particularly in the ring 1 injection kicker and in the ring 2 septum magnet, and therefore it is essential to minimise the horizontal emittance through a good betatron matching to the PS.

As the beta values depend on the radial position of the orbit, it was necessary to calculate the beta values in the septum on the trajectory of the incoming beam, rather than to use the beta values on the central orbit or injection orbit. The AGS⁵⁾ program was modified to perform a reversed tracking, starting at the junction of the incoming beam trajectory and the ring orbit (i.e. in the injection kicker) back to the entrance of the septum at the nominal radial position of the incoming beam (- 100 mm w.r.t. the centre line). A trajectory associated with the momentum deviation of the injection orbit and making an angle exactly opposite to the one made by the kicker was traced through the relevant ISR magnets and then the transfer matrices were computed for the betatron oscillation along this trajectory. In this process the multipole components of the main magnets introduced in AGS to create the working line were used (this is only an approximation because this representation applies strictly only down to a position of about - 50 mm in the D magnets) and it was checked that the influence of the gradient and field defects in the QT magnet involved in this tracking was negligible. The obtained values were used as input in the matching program MATCH¹⁴⁾, which optimises the gradients of the six most downstream BT quadrupoles.

By using these quadrupole settings, rather than the standard values (so far used on all magnetic ISR machines) a horizontal blow-up of 20 % could be eliminated. This was confirmed by transverse Schottky measurements¹⁵⁾.

REFERENCES

1. A. Verdier, Revised superconducting scheme for the ISR, CERN ISR-BOM/77-57, (1977).
2. T. Risselada and A. Verdier, Improved calculation for off-momentum orbits with the AGS program, CER ISR-BOM-OP/79-38, (1979).
3. R. Perin, T. Tortschanoff and R. Wolf, Magnetic design of the superconducting quadrupole magnets for the ISR high luminosity insertion, CERN ISR-BOM/79-2, (1979).
4. B. Autin, Influence des tolérances magnétiques sur la fonction B, application à un schéma à haute luminosité dans les ISR, CERN ISR-MA/73-29, (1973).
5. E. Keil, Y. Marti, B.W. Montague and A. Sudboe, AGS, The ISR computer program for synchrotron design, orbit analysis and insertion matching, Yellow report CERN 75-13 (1975).
6. T. Risselada et al., The CERN ISR collimator system, IEEE trans. on Nuclear Science, Vol. NS-26, no. 3, June 1979.
7. POCO, program description, T. Risselada, private communication.
8. G. Guignard, QPQQ program, private communication.
9. A. Verdier, Linear optics design of the superconducting low-B insertion in the intersecting storage rings at CERN, to be published in Nuclear Instruments and Methods in Physics Research.
10. P.J. Bryant, D.M. Lewis, B. Nielsen, B. Zotter, On-line correction of the incoherent tune shift due to space charge, ISR-MA/75-54 (1975).
11. TUCO, program description, L. Vos, private communication.
12. INCO, program description, P.P. Martucci, private communication.
13. CINE, program description, T. Risselada, private communication.
14. MATCH, program description, L. Vos, private communication.
15. J.P. Koutchouk, private communication.

A P P E N D I X 1

Analytic calculation of the transfer matrix for a transition region
with a gradient decreasing to zero

Let s be the coordinate along the closed orbit and x the transverse displacement of the particles w.r.t. the closed orbit. x is determined by the differential equation:

$$x'' + K(s) x = 0 \quad (1)$$

where $K(s)$ takes the form:

$$K(s) = K_0 \left[1 + a(s/l)^2 + b(s/l)^3 + c(s/l)^4 \right] \quad (2)$$

K_0 is the constant value inside the magnet; the parameters a , b and c describe the variation of K/K_0 from 1 for $s = 0$ to 0 for $s = l$, with $K'(0) = 0$. Imposing furthermore that:

$$K'(l) = 0 \quad \text{and} \quad \int K(s) ds = K_0 l_{\text{ext}}$$

we obtain, putting $R = l_{\text{ext}}/l$

$$a = 30R - 18 \quad b = 32 - 60R \quad c = 30R - 15$$

For the case of the SL quadrupoles l_{ext} was taken equal to 0.175 and l equal to 0.33. The associated function $K(s)$ given by (2) with

$$a = - 2.090909... \quad b = 0.181818... \quad c = 0.909090...$$

is shown in Fig. 1 and fits the computed variation well.

Equation (1) can be solved approximately by looking for a power series:

$$x(s) = x_0 + x_1s + x_2s^2 + \dots + x_n s^n$$

where the x_i 's are constants.

Putting this expansion in (1) gives:

$$2x_2 + 6x_3s + \dots + n(n-1) x_n s^{n-2} + \dots + K_0 \cdot \left[1 + a(s/l)^2 + b(s/l)^3 + c(s/l)^4 \right] \cdot \left[x_0 + x_1s + \dots + x_n s^n \right] = 0 \quad (3)$$

We now have to look for particular solutions since the elements m_{ij} of the transfer matrix are particular solutions of (1) such that:

$$m_{11}(0) = 1 \quad m'_{11}(0) = 0 \quad m_{12}(0) = 0 \quad m'_{12}(0) = 1$$

Function m_{11}

The above initial conditions are $x_0 = 1$ $x_1 = 0$, then the other terms of the series in (3) are made to vanish:

$$\text{constant terms: } 2x_2 + K_0 = 0 \quad x_2 = - K_0/2$$

$$\begin{aligned}
 \text{terms with } s & : 6x_3 = 0 & x_3 & = 0 \\
 \text{terms with } s^2 & : 12x_4 + K_0(x_2 + ax_0/l^2) = 0 & x_4 & = (K_0/12)(K_0/2 - a/l^2) \\
 \text{terms with } s^3 & : 20x_5 + K_0(x_2 + ax_0/l^2) = 0 & x_5 & = -K_0b/l^3 \\
 \text{terms with } s^4 & : 30x_6 + K_0(x_4 + x_2a/l^2 + x_1b/l^3 + x_0c/l^4) = 0 \\
 & & x_6 & = (-K_0/30)(K_0^2/24 - 7aK_0/12l^2 + c/l^4)
 \end{aligned}$$

If the calculation is stopped here, the term in K_0l^2 of the expansion of the function $K(s)$ is exactly obtained and we know that the error on the expansion is of the order of the next term which is $K_0^2l^4$. Thus we get:

$$\begin{aligned}
 m_{11}(s) = 1 - K_0l^2 \cdot \left[(s/l)^2 + a(s/l)^4/6 + b(s/l)^5/10 + c(s/l)^6/15 \right] / 2 \\
 + \text{terms of order larger than } K_0^2l^4
 \end{aligned}$$

making $s = l$, we obtain the approximate term of the matrix transfer of the transition region of length s :

$$\begin{aligned}
 m_{11} & = 1 - K_0l^2 \cdot \left[1 + a/6 + b/10 + c/15 \right] / 2 + \dots \\
 & = 1 - K_0l^2 (R - 0.2)/2
 \end{aligned}$$

for the SL case $R = 0.530303\dots$, this gives $m_{11} = 0.9837$. We notice that the first term of the expansion looks like that of the expansion of the cosine function with a correction term smaller than 1 depending on a , b and c , thus the next term can be expected to be at the most $K_0^2l^4/24$ with a correction term, which means that the error on the value of m_{11} is of the order of $K_0^2l^4/24$ i.e. 10^{-4} . The accuracy of the gradient measurement is about $1^\circ/\circ$ and therefore m_{11} is known within about the same accuracy: in this respect the accuracy of 10^{-4} of the present computation is largely sufficient.

Function m_{12}

The above initial conditions are $x_0 = 0$ $x_1 = 1$. Then the same equations as above can be used, they give:

$$m_{12}(s) = s \left[1 - K_0l^2 \cdot \left[(s/l)^2/6 + a(s/l)^4/20 + b(s/l)^5/30 + c(s/l)^6/42 \right] \right]$$

for $s = l$, we obtain:

$$\begin{aligned}
 m_{12} & = l \left[1 - K_0l^2(1/6 + a/20 + b/30 + c/42) + \text{terms of order larger than } K_0^2l^4 \right] \\
 & = l \left[1 - K_0l^2(3R - 1/3)/14 + \dots \right]
 \end{aligned}$$

For the SL case $m_{12} = 0.3287$

The functions $m_{21}(s)$ and $m_{22}(s)$ are the respective derivatives of $m_{11}(s)$ and $M_{12}(s)$ which lead to:

$$\begin{aligned}
 m_{21} & = -K_0l(1 + a/3 + b/4 + c/5) + \dots = -K_0l_{ext} + \dots \\
 & = -K_0lR
 \end{aligned}$$

the first term of this expansion is exactly the same as the term which is obtained in the hard edge approximation. This is quite normal since it is the focusing term.

$$m_{22} = 1 - K_0 l^2 (1/2 + a/4 + b/5 + c/6) + \dots$$

$$= 1 - K_0 l^2 (R - 1/5)/2 + \dots$$

This expansion still looks like a cosine as for m_{11} but the correction term is different from the one above.

The determinant of the approximate transfer function is:

$$m_{11} m_{22} - m_{12} m_{21} = [1 - K_0 l^2 (R + 1/5)/2] \cdot [1 - K_0 l^2 (R - 1/5)/2]$$

$$+ 1 \cdot [1 - K_0 l^2 (3R - 1/3)/14] \cdot [K_0 l R]$$

$$= 1 + \text{terms of the order } K_0^2 l^4$$

which is consistent with the approximation of the expansions.

Comparison between the different transfer matrices of the quadrupole end
(vertical plane)

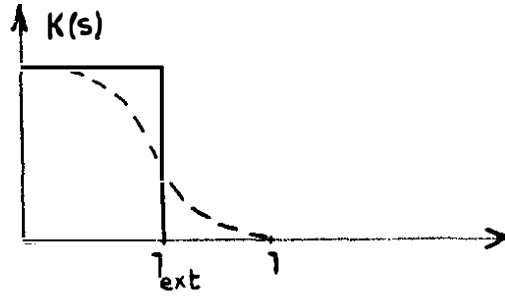
	m_{11}	m_{12}	m_{21}	m_{22}
Hard edge*	0.9937	0.3287	- 0.0716	0.9826
End in 6 pieces	0.9842	0.3287	- 0.0715	0.9922
Above calculation	0.9837	0.3287	- 0.0717	0.9926

* see Appendix 2

A P P E N D I X 2

Transfer matrix of a quadrupole end in the hard edge approximation

The gradient variation is shown below:



l is the length over which the gradient varies substantially (see Appendix 1), l_{ext} is such that:

$$K_0 l_{\text{ext}} = \int_0^l K(s) ds$$

where $K(s)$ is the actual gradient (see Appendix 1).

The transfer matrix from the origin to the point of abscissa $s = l$ is obtained from the product:

$$\begin{pmatrix} 1 & l - l_{\text{ext}} \\ 0 & 1 \end{pmatrix} \times \begin{pmatrix} C & S \\ -KS & C \end{pmatrix}$$

where $C = 1 - \frac{Kl_{\text{ext}}^2}{2} + \dots$

$$S = l_{\text{ext}} \left[1 - \frac{Kl_{\text{ext}}^2}{2} + \dots \right]$$

The expansion of the matrix elements is, putting $R = \frac{l_{\text{ext}}}{l}$

$$m_{11} = 1 - \frac{Kl^2}{2} (R^2 - 2 + 2R) + \dots$$

$$m_{12} = l \left[1 - \frac{Kl^2 R^2}{2} (3 - 2R) + \dots \right]$$

$$m_{21} = -KR \left(1 - \frac{Kl^2 R^2}{6} + \dots \right)$$

$$m_{22} = 1 - \frac{Kl^2 R^2}{2} + \dots$$

A P P E N D I X 3

Maximum excursion of a trajectory in a focusing quadrupole

Let us consider a trajectory on the axis starting at a distance d of a quadrupole, with a slope x' .

At the entrance of the quadrupole, the position and slope are respectively:

$$x'd \quad \text{and} \quad x'$$

The position inside the quadrupole is:

$$dx' \cos \sqrt{K} s + \frac{x'}{\sqrt{K}} \sin \sqrt{K} s$$

where K is the gradient divided by the rigidity ($B\rho$) of the particle and s is the longitudinal coordinate with the origin at the beginning of the quadrupole.

The slope inside the quadrupole is:

$$- dx' \sqrt{K} \sin \sqrt{K} s + x' \cos \sqrt{K} s = x' (-d \sqrt{K} \sin \sqrt{K} s + \cos \sqrt{K} s)$$

The slope can be zero inside the quadrupole, i.e. the trajectory can have an extremum x_m , if s_m exists smaller than 1, the length of the quadrupole, such that:

$$\text{tg } \sqrt{K} s_m = \frac{1}{d \sqrt{K}}$$

Which can be expressed as:

$$s_m = \frac{1}{\sqrt{K}} \text{Arctg } \frac{1}{d \sqrt{K}} \quad 1$$

For the case of a trajectory starting at the centre of the AFM, we have for the vertically focusing quadrupoles adjacent to the intersection point:

- in the outer arc:

$$d = 2.9 \text{ m} \quad K = 0.41 \text{ m}^{-2} \quad s_m = 0.77 \text{ m} \quad x_m = 3.29 x'$$

- in the inner arc:

$$d = 3.97 \text{ m} \quad K = 0.365 \text{ m}^{-2} \quad s_m = 0.65 \text{ m} \quad x_m = 4.30 x'$$

As both s_m are smaller than the quadrupole lengths which are 1.15 m, the extremum of the trajectories occur inside the quadrupoles. For the AFM, $x' = 3.7 \cdot 10^{-4}$ rad, hence the maximum vertical excursion of the orbit due to the AFM is smaller than 1.6 mm at 26 GeV.

A P P E N D I X 4

Computation of a local compensation of a dipole defect
by means of two trajectory measurements

Let x_{1i} be the trajectory positions measured at the pick up stations in a reference (or unperturbed) machine. In the ISR this can be either a single turn measurement, which is a trajectory, or a closed orbit measurement.

Let us introduce a dipole defect at a certain position; the measured trajectory positions become x_{2i} .

If we assume that $x_{2i} - x_{1i}$ is a betatron oscillation around the reference trajectory, it is possible to find two dipoles A and B which give the kicks θ_A and θ_B such that

$$\theta_A \sqrt{B_{Ai}} \sin(\mu_i - \mu_A) + \theta_B \sqrt{B_{Bi}} \sin(\mu_i - \mu_B) + (x_{2i} - x_{1i}) = 0$$

which we will write for any i

$$A_i \theta_A + B_i \theta_B + x_i = 0 \quad (1)$$

The best way to compute θ_A and θ_B is to make a "least square fit" of equation (1), which means that:

$$\sum_i \left[\theta_A \sqrt{B_{Ai}} \sin(\mu_i - \mu_A) + \theta_B \sqrt{B_{Bi}} \sin(\mu_i - \mu_B) + (x_{2i} - x_{1i}) \right]^2 = S(\theta_A, \theta_B)$$

is minimum. The condition that this function $S(\theta_A, \theta_B)$ is minimum is expressed by:

$$\frac{\partial S}{\partial \theta_A} = \frac{\partial S}{\partial \theta_B} = 0$$

The solution of this system is:

$$\theta_A = \frac{(\sum B_i^2)(\sum A_i X_i) - (\sum A_i B_i)(\sum B_i X_i)}{(\sum A_i B_i)^2 - (\sum A_i^2)(\sum B_i^2)}$$

$$\theta_B = \frac{(\sum A_i^2)(\sum B_i X_i) - (\sum A_i B_i)(\sum A_i X_i)}{(\sum A_i B_i)^2 - (\sum A_i^2)(\sum B_i^2)}$$

A P P E N D I X 5

1. Motion in the "phase space"

The amplitude $y(s)$ of the betatron oscillation at the position s in a machine is given by:

$$y(s) = \sqrt{E B(s)} [\sin \mu(s) + \varphi]$$

where E and φ are constants depending on the value of x and its derivative at a given position. The amplitude function $B(s)$ and the phase advance $\mu(s)$ depends only on the machine geometry and on the normalized gradients (i.e. the gradients divided by the rigidity of the particles).

The normalized coordinate:

$$x(s) = y(s) / \sqrt{B(s)} = \sqrt{E} \sin [\mu(s) + \varphi]$$

is therefore a pure sinusoidal function. Its derivative w.r.t. μ is

$$x'_\mu(s) = \sqrt{E} [\cos \mu(s) + \varphi]$$

If the betatron motion is represented in the phase plane x x'_μ , the trajectories are circles of radius \sqrt{E} and $dx'_\mu(s)/d\mu$ always has its sign opposite to that of $x(s)$ which means that the motion of the point of coordinates $x(s)$, $x'_\mu(s)$ occurs clockwise.

2. Representation of an aperture restriction

Let us consider two particles A and B with the same emittance E going from a point 1, to a point 2 where particles with an amplitude larger than x_2 (positive) are eliminated by the aperture restriction.

The motion is sketched in Fig. 5.

In this particular case particle B is eliminated at point 2.

The same representation as Fig. 2 b can be obtained by rotating this Figure anticlockwise by $\Delta\mu$, the phase advance between point 2 where the aperture restriction occurs and point 1 which is the origin of the motion.

Thus it is only necessary to specify the coordinates of the particles at point 1: the eliminated particles are obtained without considering the betatron motion as shown in Fig. 5 c.

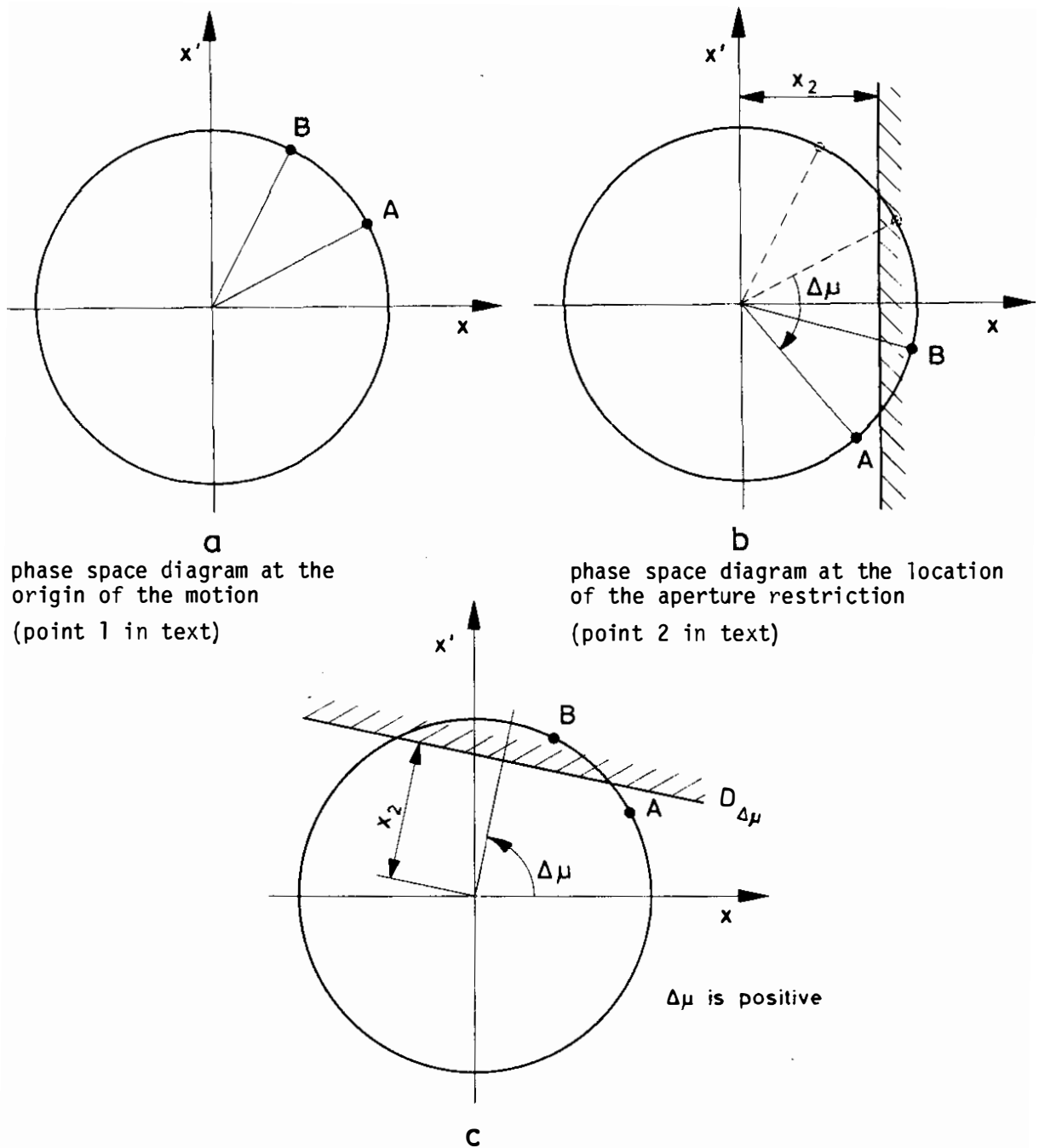


Fig. 5: Representation of an aperture restriction located at the phase $\Delta\mu$ w.r.t. the particles in the positions A and B.

For a given machine which has a continuous vacuum chamber, a straight line $D_{\Delta\mu}$ is associated with every point of the vacuum chamber at the phase $\Delta\mu$ w.r.t. an arbitrary origin. This ensemble has an innermost envelope. This envelope represents the aperture restriction over the number of turns for which it is traced.

3. Application to the case of two collimators

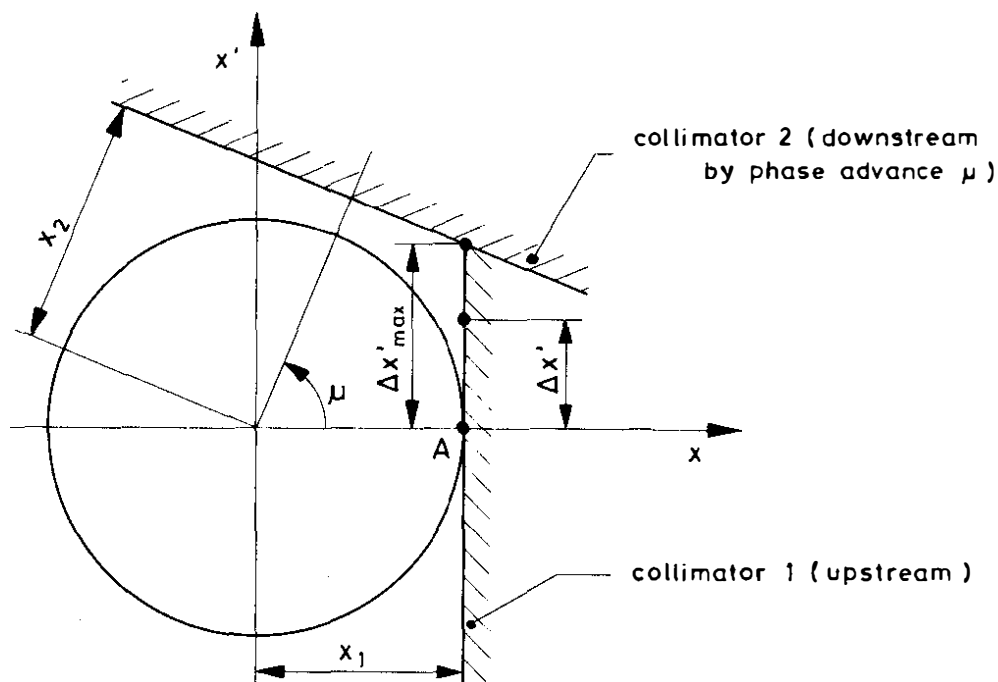


Figure 6

Let us take the origin of the phase at the upstream collimator; let us assume that there is no other aperture restriction. Collimator 1 is set as an aperture limitation defined by the distance x_1 from which the closed orbit under consideration is distant. Particles are deflected by collimator 1 so that their representing point is not A but is displaced vertically by $\Delta x'$. For any $\Delta x' < 0$ the deflected particles miss collimator 2. For $\Delta x' > 0$ there exists a value $\Delta x'_{\max}$ below which the deflected particles miss collimator 2 and beyond which they are stopped (Fig. 6).

If we now consider an infinite number of turns of the particles, collimator 1 has to be set at all phases $\mu = n(2\pi/Q)$ where n is any integer. The envelope of the straight lines representing collimator 1 is therefore the circle of radius x_1 which implies that a particle that has been deflected once will be stopped later on.

In such phase space plots the available aperture of a machine can be evaluated. The data are calculated by the program TOUCH (author K. Brand). This program calculates for a given part of a machine, or for a complete turn around the machine, the acceptance of the vacuum chamber for a given orbit.

The calculated acceptance is plotted in a phase space plot by the program MUSCAT (author T. Risselada). Aperture restrictions (for example collimators) may then be introduced and plotted in the same plot. The program may also be requested to calculate angular distributions of protons scattered by multiple scattering in a given collimator, scraper, septum, etc. and to plot their population in the phase space plot.

The circulating beam envelope is indicated by a circle with area equal to 9 times the beam emittance (this number is based on practical experience with collimator systems), and the collimators may be automatically set by the program against this circle. The orbit coordinates and betatron parameters are computed by the AGS program. This allows evaluation of a given collimator system on different machine optics and different $\Delta p/p$ values.

Table 4 c

Ring 2 - Summary of the AGS output for the central orbit (linear scheme)

Table with columns: NO, ELEM, L(M), ANG(MR), K(1/M2), BETA(M), BETA(M), ALPHAV, ALPHA, MUW/2PI, MUH/2PI, ALPHAP(M), ALPHAP. Includes sub-headers for SUP. COND. LOWIICIA SCHEME, R2, I8, STANDARD SFM, GL WITH END EFFECTS; IGRAGG 75.03; 24/10/80 17.34.50; CIRCUMFERENCE 9.4263610; SUPERPERIODS 1; STRAIGHT MAGNETS; ALL VALUES AT EXIT OF ELEMENTS. The table contains a large list of numerical data points for various elements.

OP/P COSMU(H) Q(H) QPRIME(H) BETA MAX(H) COSMU(V) Q(V) QPRIME(V) BETA MAX(V) X MAX(H) GAMMA TR.
0.0000 0.1634 8.9020 -17.5839 117.6030 7.7350 0.8020 -14.8868 69.7756 2.3061 8.9264
UP/P 0.0000 AVERAGE X = 0.0000 AVERAGE ALPHA P = 1.0028 R. P. GAMMA TR = 0.9264

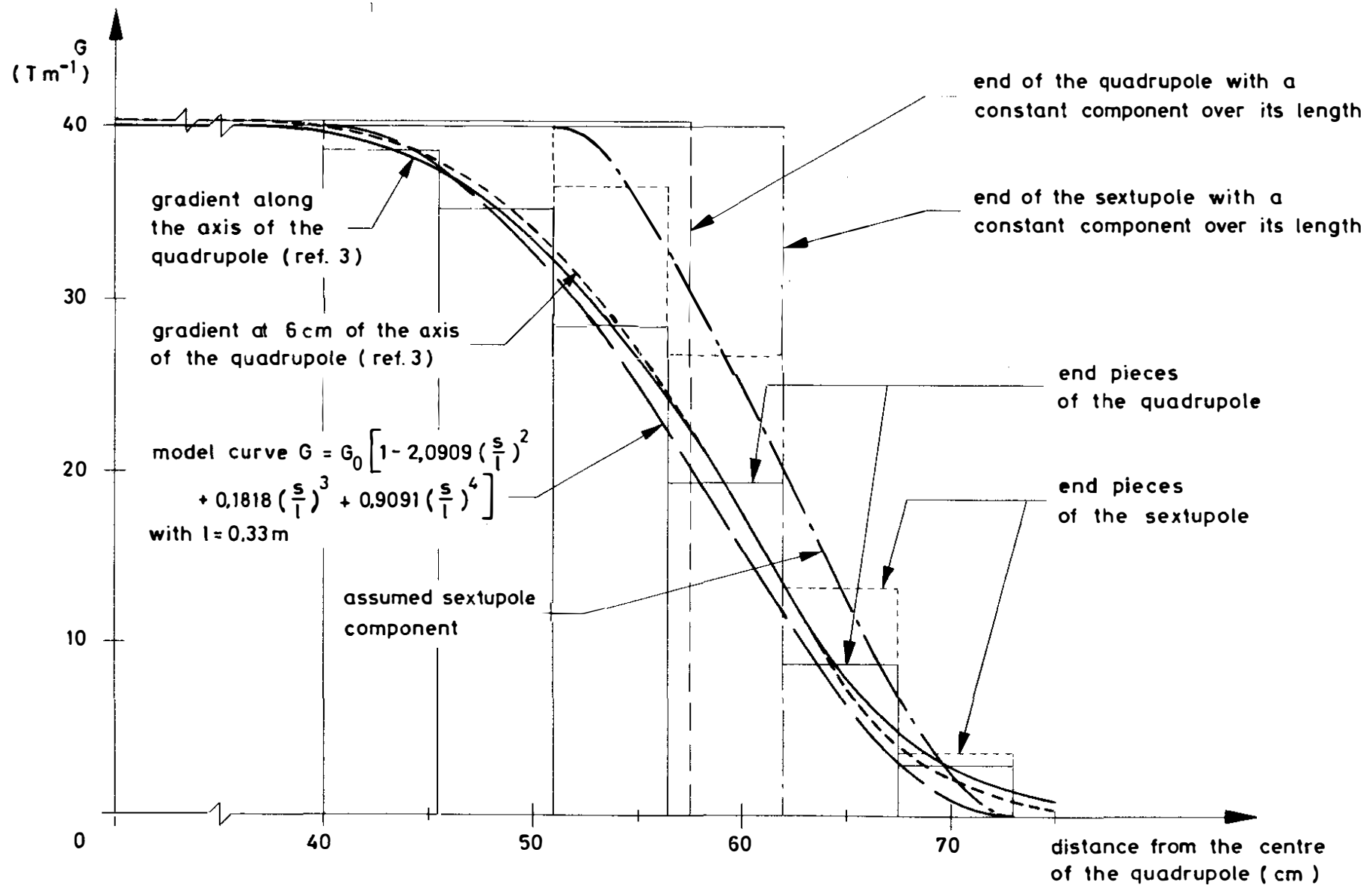


Fig. 1: Longitudinal variation of the gradient (computed Ref. 3, Fig. 11) and of the sextupole component (assumed) at the superconducting quadrupole ends. The step functions used for the AGS description are represented, the details are explained in paragraph 1.2.

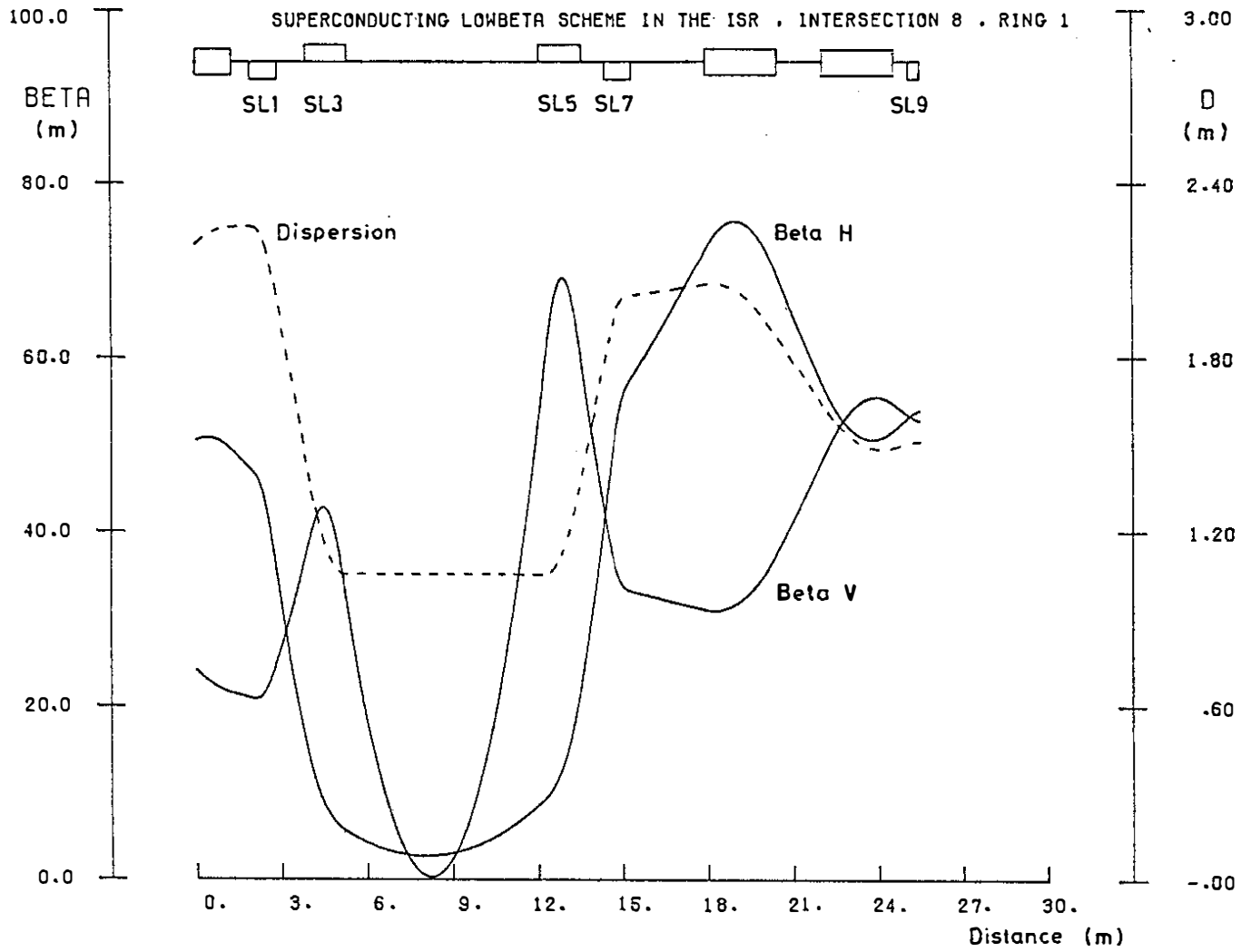


Fig. 2: Beta functions and dispersion inside the superconducting low- β insertion of the ISR in ring 1. SL1, 3, 5, 7 are superconducting quadrupoles, SL9 is a conventional quadrupole. Non referenced magnets are ISR main magnets.

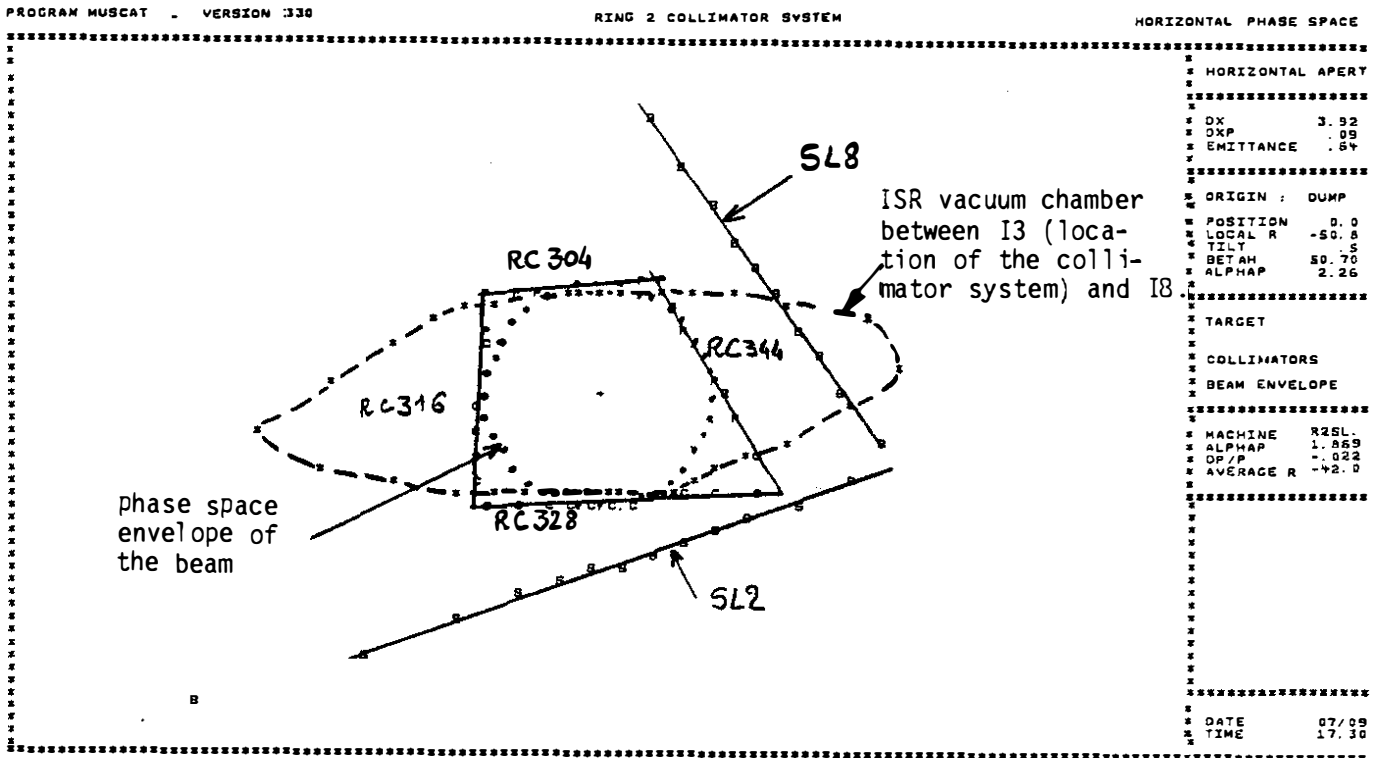
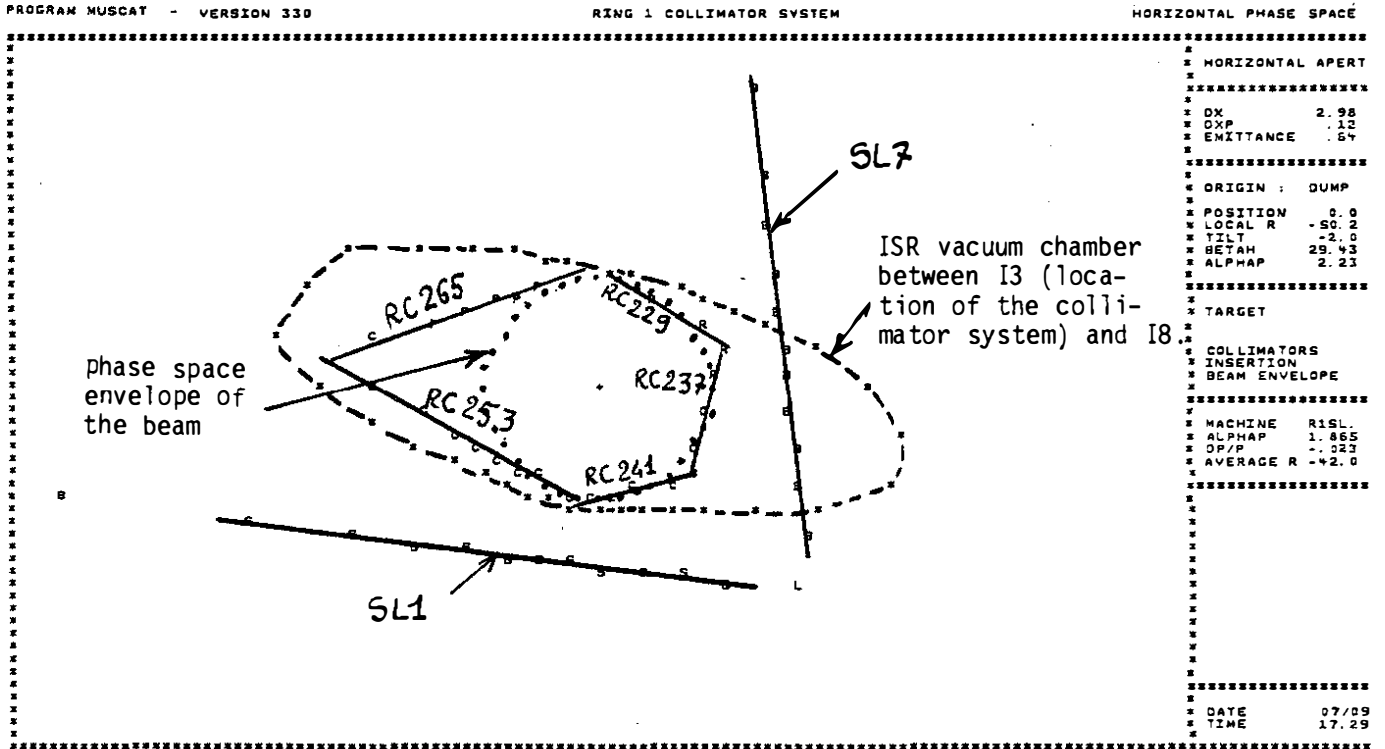


Fig. 3: Phase-space plots on the injection orbit for evaluation of the protection of I8 by the collimator system and the vacuum chamber downstream from it.

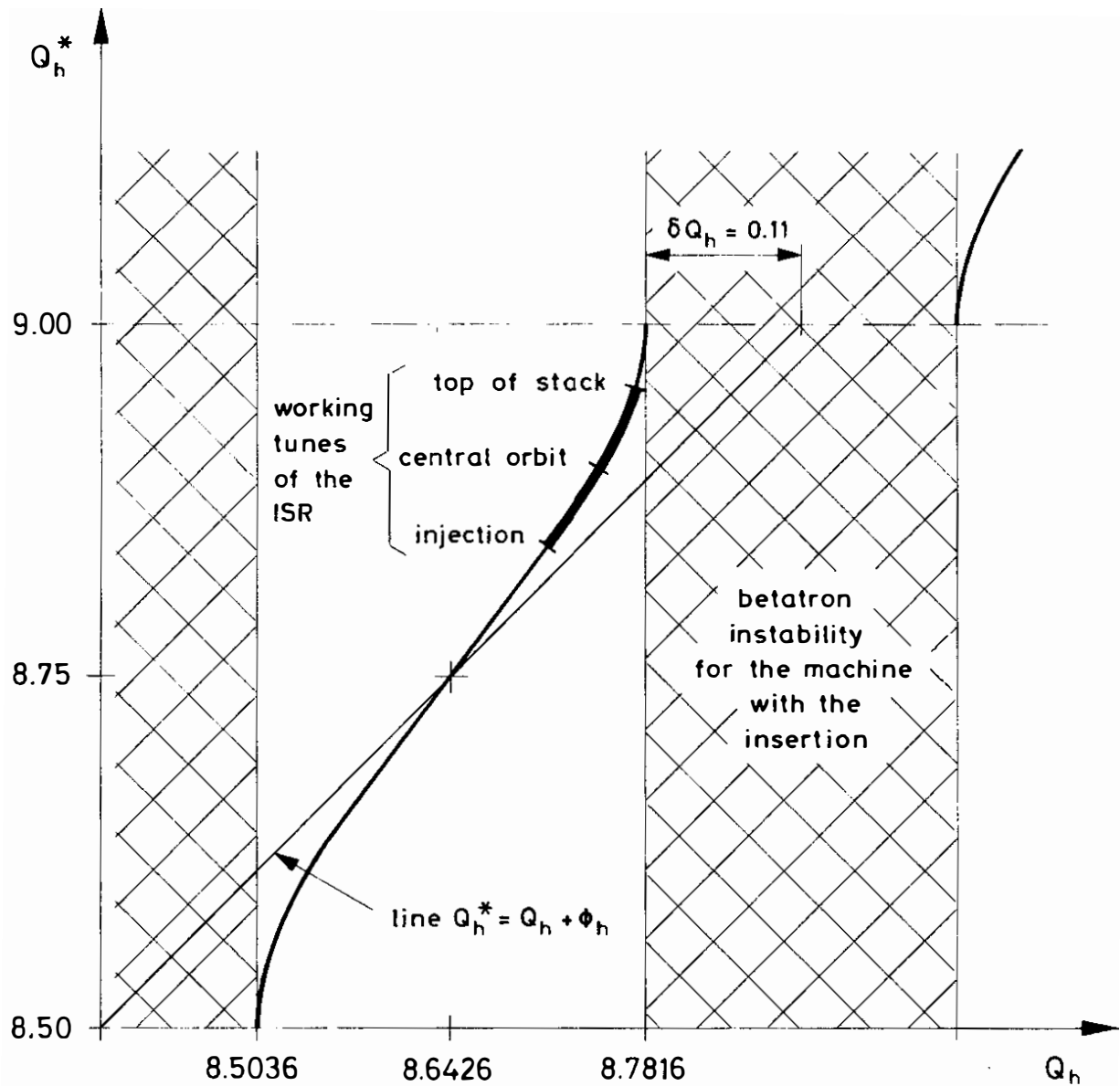


Fig. 4: Horizontal tune of the SL machine Q_h^* as a function of the tune of the base machine Q_h according to the formula

$$\cos 2\pi Q_h^* = \cos 2\pi (Q_h + \phi_h) / \cos 2\pi \delta Q_h.$$

Since Q_h is a smooth function of gradients, this picture shows the gradient stopbands due to the SL insertion.

$$\phi_h = 0.1074 \quad \delta Q_h = 0.111$$

If the insertion were perfectly matched, δQ_h would be zero and we would have $Q_h^* = Q_h + \phi_h'$.

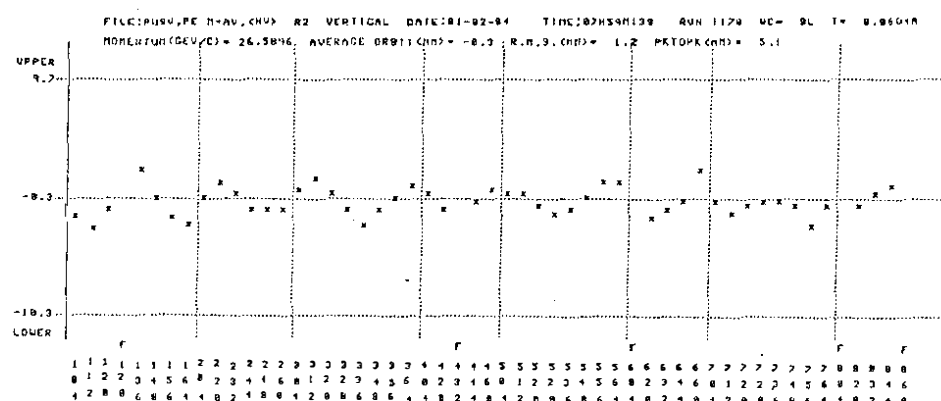
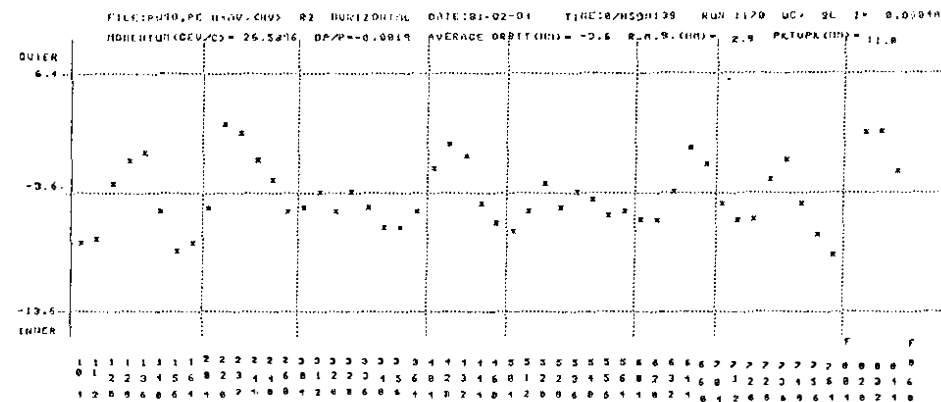
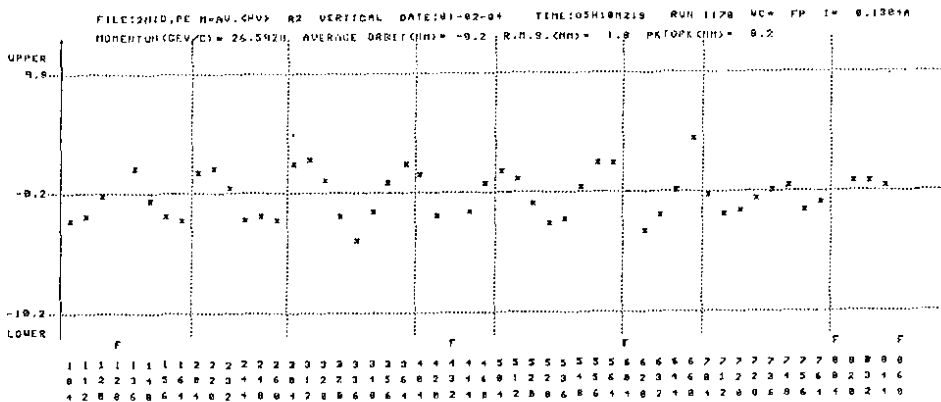
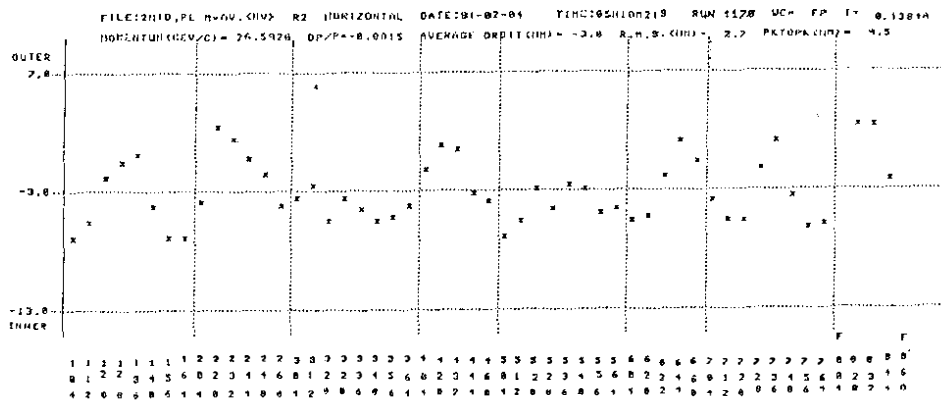


Fig. 5: Measurement of the position of the central closed orbit before turning on the SL insertion i.e. on the BASE machine (two upper plots) and after turning on the SL insertion and making a local compensation by INCO (two lower plots). Explanations in para. 2.5.